



**HAL**  
open science

# Calibration of a productivity model for the microalgae *Dunaliella salina* accounting for light and temperature

Quentin Béchet, Philippe Moussion, Olivier A. Bernard

## ► To cite this version:

Quentin Béchet, Philippe Moussion, Olivier A. Bernard. Calibration of a productivity model for the microalgae *Dunaliella salina* accounting for light and temperature. *Algal Research - Biomass, Biofuels and Bioproducts*, 2017, 21, pp.156 - 160. 10.1016/j.algal.2016.11.001 . hal-01410980

**HAL Id: hal-01410980**

**<https://inria.hal.science/hal-01410980>**

Submitted on 27 Jan 2017

**HAL** is a multi-disciplinary open access archive for the deposit and dissemination of scientific research documents, whether they are published or not. The documents may come from teaching and research institutions in France or abroad, or from public or private research centers.

L'archive ouverte pluridisciplinaire **HAL**, est destinée au dépôt et à la diffusion de documents scientifiques de niveau recherche, publiés ou non, émanant des établissements d'enseignement et de recherche français ou étrangers, des laboratoires publics ou privés.



Distributed under a Creative Commons Attribution 4.0 International License

1 Calibration of a productivity model for the microalgae

2 *Dunaliella salina* accounting for light and temperature

3

4 Quentin Béchet<sup>a,b\*</sup>, Philippe Moussion<sup>a,b</sup>, Olivier Bernard<sup>a,b</sup>

5

6 <sup>a</sup> Université Côte d'Azur, Inria, BIOCORE, BP 93 06902 Sophia Antipolis Cedex, France

7 <sup>b</sup> Sorbonne Universités, UPMC Université Paris 06, CNRS, UMR 7093, LOV, Observatoire  
8 océanologique, F-06230, Villefranche/mer, France

9

10 \* Corresponding author

11 Telephone: +33 4 92 38 71 74

12 Fax: + 33 4 92 38 78 58

13 Email: [quentin.bechet@inria.fr](mailto:quentin.bechet@inria.fr)

14 Abstract

15

16 This study aimed to calibrate a productivity model for the algal species *Dunaliella salina*  
17 accounting for the impacts of light intensity and temperature. The calibration was performed  
18 by using a dedicated experimental set-up measuring short-term oxygen production rates at  
19 different light intensities. The rate of photosynthesis was shown to follow a typical Monod  
20 function of light intensity. The slope of Photosynthesis-light curves at low light intensity was  
21 also shown to be independent on temperature and the evolution of model parameters with  
22 temperature obeyed relationships consistent with previous observations in the literature.  
23 Finally, the rate of respiration was shown to follow an Arrhenius function of temperature.  
24 This good level of agreement with prior observations in the literature indirectly validates the  
25 experimental technique used for model calibration. The resulting model should therefore yield  
26 accurate productivity predictions in outdoor cultivation systems.

27

28 Keywords: Algae; *D. salina*; growth kinetics; productivity model; photosynthesis; respiration

29 1. Introduction

30 With the objective to accurately assess the economical and environmental feasibility of full-  
31 scale algal cultivation for biofuel production, a large number of studies developed  
32 mathematical models predicting algal productivity in outdoor cultivation systems [1–3].  
33 These models can be used to improve process design or develop optimization strategies  
34 maximizing algal productivity. For instance, Slegers et al. [4] used a mathematical model  
35 predicting growth rates of *Phaeodactylum tricornutum* and *Thalassiosira pseudonana* to  
36 optimize the design of closed photobioreactors. Similarly, Béchet et al.[5] proposed an  
37 optimization strategy based on the dynamic control of pond depth and hydraulic retention  
38 time to increase productivity while reducing water demand, using a productivity model for  
39 *Chlorella vulgaris*. Alternatively, adapting the algal species to climatic conditions could  
40 potentially boost yearly algal productivity, similarly to crop rotation used in traditional  
41 agriculture. For example, algal species having low optimal temperatures could be cultivated in  
42 colder climates or simply during winter while heat-resistant algal species could be grown in  
43 summer when pond temperature reaches higher levels. With the objective to assess the  
44 benefits of these 'algal culture rotation' strategies, it is necessary to calibrate algal productivity  
45 models for a large number of species. However, while many studies in the literature  
46 developed productivity models, these models have been calibrated on a limited number of  
47 algal species. In particular, the impact of temperature was often neglected in past studies,  
48 which limits models application to outdoor systems where temperature significantly varies  
49 [1].

50

51 Within this context, our research group has been developing mathematical models to predict  
52 algal productivity in various outdoor cultivation systems from meteorological hourly data,  
53 system design and operation. This modeling framework combined models predicting system

54 temperature with a biological model predicting algal productivity as a function of light and  
55 temperature. So far, the biological model has only been calibrated for a single algal species,  
56 *Chlorella vulgaris* (see Béchet et al. [6]). The objective of this study was therefore to calibrate  
57 a productivity model for another algal species, *Dunaliella salina*, this species being the third  
58 most cultivated microalgae [7]. *Chlorella vulgaris* and *Dunaliella salina* are both  
59 Chlorophyceae and share the same tolerance to high temperatures. The methodology followed  
60 in this study was therefore similar to the calibration technique followed by Béchet et al. [6],  
61 and also because the model for *C. vulgaris* accurately predicted productivities in indoor  
62 (accuracy of +/- 15% over 163 days; Béchet et al. [6]) and outdoor (accuracy of +/- 8.4% over  
63 148 days, Béchet et al. [8]) reactors.

## 64 2. Materials and methods

### 65 2.1. Algae cultivation conditions and biomass characterization

66 The Chlorophyceae *Dunaliella salina* (CCAP 19/18) was cultivated in a cylindrical  
67 photobioreactor (diameter: 0.19 m; height: 0.41 m; culture volume: 10 L; gas phase volume:  
68 1.6 L). The reactor was illuminated by two metal halide lamps (Osram Powerstar HQI-TS,  
69 150W NDL, Neutralweiss de Luxe) providing a light intensity of 1440  $\mu\text{mol}/\text{m}^2\text{-s}$  (measured  
70 when the reactor was filled with water with a QSL-2100 PAR scalar irradiance sensor,  
71 Biospherical Instruments). Temperature was maintained at 30°C by re-circulating  
72 temperature-controlled water in a jacket around the reactor. The reactor was inoculated with a  
73 culture of *D. salina* (inoculum volume of approximately 500 mL) grown in axenic conditions  
74 (light intensity: 300  $\mu\text{mol}/\text{m}^2\text{-s}$ , light-dark cycle: 12:12, temperature: 27°C) and was then  
75 operated as a fed-batch system: 9L of solution was replaced every week with fresh f/2  
76 medium [9] enriched in phosphorus and nitrogen to ensure that algal growth was not limited  
77 by nutrients (Total N and P concentrations in enriched medium: 0.22 g N-NO<sub>3</sub><sup>-</sup>/L; 0.020 g P-

78  $\text{PO}_3^-/\text{L}$ ). Air enriched in  $\text{CO}_2$  (2%  $\text{CO}_2$ ) was continuously bubbled in the photobioreactor to  
79 ensure that  $\text{CO}_2$  supply did not limit algal growth and also to control pH between 7 and 7.5.  
80 Algae used for model calibration were extracted from the photobioreactor 2-3 days after  
81 medium change during the light-limited growth phase. The biomass concentration in the  
82 solution used during model calibration was measured by dry weight [10]. Glass-fiber filters  
83 (GF/C, Whatman, diameter: 25mm, No 1822-025) were first dried for several days at 60°C  
84 before being weighed. A known volume of the algal solution was then filtered; filters were  
85 then rinsed with Ammonium formate (30 g/L) to remove salt. Filters were then dried for 24  
86 hours at 60°C before being weighed again. Dry weight concentration was measured in  
87 duplicates.

88

## 89 2.2. Productivity model description

90 Algal productivity ( $P_{net}$ , in  $\text{kg O}_2/\text{s}$ ) was expressed as the difference between the gross rate of  
91 photosynthesis ( $P$ , in  $\text{kg O}_2/\text{s}$ ) and the rate of endogenous respiration ( $ER$ , in  $\text{kg O}_2/\text{s}$ ) [6]:

$$92 P_{net} = P - ER \quad (1)$$

93 The gross rate of photosynthesis was expressed as a function of light intensity and  
94 temperature by using a 'type-II model' as recommended by Béchet et al. [1]. This type of  
95 models is based on the assumption that the local rate of photosynthesis of single algal cells  
96 can be expressed as a direct function of the local light intensity cells are exposed to. Béchet et  
97 al. [6] used different formulas to express local rates of photosynthesis as a function of local  
98 light intensity and showed that the three formulas most commonly used in the literature all  
99 satisfyingly fit experimental data. The authors finally selected the Monod formula, as this  
100 expression was the most commonly found in literature. The gross rate of photosynthesis was  
101 therefore expressed as [6]:

102 
$$P_{net} = \int_V P_m(T) \frac{\sigma_X I_{loc}}{K(T) + \sigma_X I_{loc}} X \cdot dV \quad (2)$$

103 where  $P_m$  is the maximum specific rate of photosynthesis (kg O<sub>2</sub>/kg-s),  $T$  is the culture  
 104 temperature (°C),  $K$  is the half-saturation constant (W/kg),  $\sigma_X$  is the extinction coefficient  
 105 (m<sup>2</sup>/kg),  $I_{loc}$  is the local light intensity (W/m<sup>2</sup>, as photosynthetically active radiation or PAR),  
 106  $X$  is the algal concentration (kg/m<sup>3</sup>) and  $V$  is the culture volume (m<sup>3</sup>). The local light intensity  
 107  $I_{loc}$  was expressed by using a Beer-Lambert law:

108 
$$I_{loc}(l) = I_0 \exp(-\sigma_X X l) \quad (3)$$

109 where  $l$  is the light path between the considered location and the reactor external surface (m)  
 110 and  $I_0$  is the incident light intensity (W/m<sup>2</sup>). The evolution of  $P_m$  and  $K$  with temperature was  
 111 fitted to the theoretical model of Bernard and Rémond [11] as this model was shown to  
 112 satisfyingly fit the evolution of the specific growth rate of 15 algal species.  $P_m$  and  $K$  were  
 113 therefore expressed as follows:

114 
$$p = \begin{cases} \alpha \frac{(T-T_{max})(T-T_{min})^2}{(T_{opt}-T_{min})((T_{opt}-T_{min})(T-T_{opt})-(T_{opt}-T_{max})(T_{opt}+T_{min}-2T))} & \text{if } T_{min} \leq T \leq T_{max} \\ 0 & \text{otherwise} \end{cases} \quad (4)$$

115 where  $p$  represents either  $P_m$  or  $K$ ,  $\alpha$  is the maximum value of  $P_m$  or  $K$ , and  $T_{min}$ ,  $T_{max}$  and  $T_{opt}$   
 116 are the minimum, maximum, and optimum temperatures for photosynthesis (°C), respectively.

117 The rate of endogenous respiration was expressed using a first-order law:

118 
$$ER = \lambda(T) X V \quad (5)$$

119 where  $\lambda$  is the specific respiration rate (kg O<sub>2</sub>/kg-s). Several studies showed that the rate of  
 120 respiration was an exponential function of temperature [12–14]. The parameter  $\lambda$  was  
 121 therefore expressed as follows:

122 
$$\lambda(T) = \lambda_0 \exp(\beta T) \quad (6)$$

123 where  $\lambda_0$  (kg O<sub>2</sub>/kg-s<sup>-1</sup>) and  $\beta$  (°C<sup>-1</sup>) are determined experimentally.

124

### 125 2.3. Device used for model calibration

126 The device used for calibration was composed of six cylindrical glass reactors (diameter: 3.48  
127 cm; height: 5.82 cm; volume: 55.2 mL) all equipped with an oxygen electrode (Model DO50-  
128 GS, Hach) measuring both dissolved oxygen and medium temperature. Each reactor was  
129 positioned over a LED lamp (12V PHILIPS EnduraLED 10W MR16 Dimmable 4000 K)  
130 which light intensity was independently controlled. A typical experiment consisted on  
131 measuring first oxygen production rates when algae were exposed to light (light-phase) and  
132 then respiration rates when algae were in the dark (dark phase). These measurements were  
133 performed for six different light intensities (range: 0-460 W/m<sup>2</sup>, as PAR) and under constant  
134 temperature (see [6] for a complete description of the oxygen measurements). These  
135 experiments were then repeated for 6 different temperatures (3.73°C; 10.2°C; 19.7°C, 27.7°C,  
136 34.7°C; 40.9°C). Temperature was maintained constant (within approximately +/- 1°C) during  
137 the entire duration of the experiment by circulating temperature-controlled air around the  
138 reactors. The light intensity reaching the external surface of each reactor was measured by  
139 actinometry (see S1 for details). The parameters  $P_m$  and  $K$  for each temperature were  
140 determined by least-square fitting using the *lsqcurvefit* Matlab function. Respiration rates  
141 during the dark periods were found to be independent on the light intensity cells where  
142 exposed to during the light phase and the parameter  $\lambda$  was determined from the average  
143 respiration rate in the six reactors. The parameters  $T_{min}$ ,  $T_{max}$ ,  $T_{opt}$ , were obtained by least-  
144 square fitting (using the *lsqcurvefit* Matlab function) and the parameters  $\lambda_0$  and  $\beta$  were  
145 estimated by log-linear regression. Algae were found to be photosynthetically inactive after  
146 exposure to 43°C for 30 min (unpublished data).  $P_m$  was therefore considered null at 43°C  
147 when determining  $T_{min}$ ,  $T_{max}$ , and  $T_{opt}$ . Based on the linear relationship between  $P_m$  and  $K$  (see  
148 section 3.1 for details),  $K$  was also assumed null at this temperature.

149



#### 150 2.4. Measurement of extinction coefficient

151 The extinction coefficient  $\sigma_X$  was experimentally determined by measuring the light  
152 intensities entering and exiting the reactors for different algal concentrations (see S2 for  
153 details). Similarly to the formula proposed by [15], the extinction coefficient was expressed as  
154 follows:

$$155 \sigma_X = AX^B \quad (7)$$

156 where  $A$  and  $B$  are empirical coefficients ( $A = 79.1$ ;  $B = -0.37$ , see S2 for details). The  
157 dependence of the extinction coefficient on algal concentration was mostly due to light  
158 scattering by algal cells. Scattered photons indeed exited the reactors through the lateral side  
159 of the reactors. This effect was reinforced by the fact that LEDs lamps did not emit light in a  
160 vertical direction but in a cone of an angle  $30^\circ$ , which increases the fraction of light lost  
161 through the reactors lateral sides. When the algal concentration increased, most of photons  
162 were absorbed by algal cells and the fraction of light exiting the reactors through the lateral  
163 sides decreased. This explains why the extinction coefficient is less sensitive to  $X$  for high  
164 algal concentrations (Equation 7; see S2 for further detail). Calibration experiments were  
165 therefore performed at relatively high algal concentrations to ensure that most of incoming  
166 light was absorbed by algae.

167

#### 168 2.5. Application to the calibration device

169 Based on Equations 1-7, the algal productivity in each reactor used for model calibration was  
170 expressed as follows:

$$171 P_{net}(T, I_0) = \frac{P_m(T)S}{\sigma_X} \ln \left( \frac{K(T) + \sigma_X I_0}{K(T) + \sigma_X I_0 \cdot \exp(-\sigma_X XL)} \right) - \lambda(T)XSL \quad (8)$$

172 where  $T$  is the culture temperature ( $^\circ\text{C}$ ),  $I_0$  is the incident light intensity at the reactor bottom  
173 ( $\text{W m}^{-2}$ ),  $P_m$ ,  $K$  and  $\lambda$  are the temperature-dependent model parameters (see Equations 4 and

174 6),  $\sigma_X$  is the extinction coefficient (see Equation 7),  $X$  is the algal concentration ( $\text{kg m}^{-3}$ ), and  
175  $L$  and  $S$  are the reactor height (m) and section surface area ( $\text{m}^2$ ), respectively.

176

## 177 2.6. Monte-Carlo simulations

178 Monte-Carlo simulations were performed to quantify the impact of experimental error on the  
179 fitted values of model parameters  $P_m$ ,  $K$  and  $\lambda$ . Namely, four key measurements were found to  
180 have a significant impact on model parameters:

- 181 - The extinction coefficient  $\sigma_X$ : coefficients  $A$  and  $B$  in Equation 7 were found to vary in  
182 the ranges 74.50-82.78 and -0.20--0.48, respectively (see S2 for details);
- 183 - The dissolved oxygen concentration: oxygen probes were found to be accurate at +/-  
184 4.7% (see S3 for details);
- 185 - The incident light intensity  $I_0$ : Measurements by actinometry were assumed to be  
186 accurate at +/-10% based on the study of Hatchard and Parker [16] (See S1 for  
187 details).
- 188 - The algal concentration  $X$ : an accuracy of +/-7% on dry weight measurements was  
189 assumed by analogy with the study of Béchet et al. [6].

190

191 In practice, the uncertainties on the parameters  $P_m$ ,  $K$  and  $\lambda$  were obtained from the following  
192 Monte-Carlo approach. Assuming that errors were normally distributed, a large artificial data  
193 set was generated by adding a normally distributed error to the measurements (algal  
194 concentration  $X$ , light intensity  $I_0$  and oxygen concentration) and the extinction coefficient  
195 ( $\sigma_X$ ). A total of 2000 artificial data sets were thus generated and the parameters  $P_m$ ,  $K$  and  $\lambda$   
196 were determined with a minimization algorithm for each data set. This approach yielded a  
197 normal distribution for  $P_m$ ,  $K$  and  $\lambda$ , which allowed determining confidence intervals for each  
198 of these parameters. These resulting confidence intervals were then used to determine levels

199 of uncertainty on the parameters  $T_{min}$ ,  $T_{max}$ ,  $T_{opt}$ ,  $\lambda_0$  and  $\beta$  through another set of Monte-Carlo  
200 simulations (see [6] for further details on Monte-Carlo simulations).

201

## 202 2.7. Conversion coefficients from oxygen to biomass productivity

203 The productivity model developed in this study predicts algal productivity in terms of oxygen  
204 (see Equations 1-6). For engineering purposes, it is however necessary to express  
205 productivities in terms of biomass. The conversion from oxygen to biomass productivities  
206 was performed by following the approach of Béchet et al. [6]. This conversion was based on  
207 the assumption of a photosynthetic quotient of 1 mole of CO<sub>2</sub> consumed for the production of  
208 1 mole of O<sub>2</sub> during the light reactions of photosynthesis, which was supported by the  
209 experimental measurement of the photosynthetic quotient of a close algal species (*Dunaliella*  
210 *tertiolecta*) by Wegmann and Metzner [17]. This photosynthetic quotient of 1 does not  
211 include respiratory mechanisms and only reflects photosynthesis. From the knowledge of  
212 algal composition and by considering that nitrate was used as a nitrogen source, the following  
213 conversion coefficients were obtained (see S4 for details):

214 -  $P_m' [\text{kg/kg-s}] = 0.75 (\pm 0.10) P_m [\text{kg O}_2/\text{kg-s}]$

215 -  $\lambda' [\text{kg/kg-s}] = 0.75 (\pm 0.10) \lambda [\text{kg O}_2/\text{kg-s}]$  at daytime

216 -  $\lambda' [\text{kg/kg-s}] = 0.9375 (\pm 0.10) \lambda [\text{kg O}_2/\text{kg-s}]$  at nighttime

217

## 218 3. Results and discussion

### 219 3.1. Rate of photosynthesis

220 Figure 1 shows that the Type-II model coupling a Monod formula with the modified Beer-  
221 Lambert law was able to describe the evolution of the rate of photosynthesis with light  
222 intensity. These PI-curves do not exhibit the typical decrease at high light intensities due to

223 photo-inhibition observed for *D. salina* in dilute cultures through chlorophyll fluorescence  
224 measurements by Combe et al. [18]. This is explained by the high algal concentration that  
225 ensured that only a small fraction of cells were photo-inhibited, so that the impact of photo-  
226 inhibition was minimal, as suggested by Bernard [19]. Experimental errors caused relatively  
227 high uncertainty on fitted values of  $P_m$  and  $K$  as shown in Table 1 and especially at the  
228 temperature of 40.9°C as the gross productivity was only measured at two light intensities (the  
229 oxygen net productivity was negative at low light intensities due to high respiration rates at  
230 this temperature, and oxygen concentration remained null during all experiment). Because of  
231 these experimental uncertainties, it was difficult to accurately identify  $P_m$  and  $K$  separately. In  
232 other words, various combinations of  $P_m$  and  $K$  could yield equally satisfying fits in Figure 1.  
233 In spite of these levels of inaccuracy, Figure 2 shows that  $P_m$  and  $K$  were correlated ( $R^2 =$   
234 0.87558), which was previously observed by Béchet et al. [6]. The ratio  $P_m/K$  indeed  
235 represents the maximum 'yield' of photosynthesis (in kg O<sub>2</sub>/W-s), i.e. the amount of oxygen  
236 produced through photosynthesis per unit light energy captured by cells. For low light  
237 intensities, this maximum yield is theoretically independent of temperature [20], which  
238 explains the linearity observed in Figure 2.

239

240 Figure 3 shows that experimental values of  $P_m$  followed a typical response to temperature  
241 characterized by a slow increase from cold to optimal temperatures before a fast drop for  
242 higher temperatures. The model of Bernard and Rémond [11] especially developed for this  
243 type of temperature response thus provides a good fit to experimental data (Figure 3).

244 Interestingly, the model of Bernard and Rémond successfully described the evolution of  $K$ ,  
245 with similar values for  $T_{min}$ ,  $T_{max}$ , and  $T_{opt}$  as shown in Table 2. This similarity is explained by  
246 the linearity between  $P_m$  and  $K$  shown in Figure 2. The values of  $T_{min}$ ,  $T_{opt}$  and  $T_{max}$  are within  
247 the range of values obtained by Bernard and Rémond [11] for 15 other algal species. The

248 value of the maximum temperature  $T_{max}$  is in the upper range of reported values for other algal  
249 species, which may be explained by two reasons. Firstly, *D. salina* is known to resist to high  
250 temperatures as this species is naturally found in shallow water bodies in which temperature  
251 can reach relatively high values [21,22]. In addition, this model calibration is based on short-  
252 term measurements of photosynthesis (approximately 30 min) while Bernard and Rémond  
253 [11] fitted their model on growth rate measurements obtained over several days of cultivation.  
254 Even if Bernard and Rémond [11] did not calibrate their model on *D. salina* data, this  
255 difference in time scales may explain the relatively high  $T_{max}$  value (43°C) as short-term and  
256 long-term algal responses are not controlled by the same biological processes. Oxygen  
257 production indeed reflects the rate of initial non-enzymatic steps of photosynthesis (usually  
258 referred to as "light reactions"), while carbon fixation through Calvin cycle and more  
259 generally growth involve enzymatic processes that are more impacted by temperatures. For  
260 example, Béchet et al. [6] showed that *Chlorella vulgaris* was unable to sustain growth at a  
261 constant temperature of 35°C for more than 1-2 hours while the oxygen productivity peaked at  
262 38°C. The uncertainty on  $P_m$  and  $K$  showed in Table 1 caused levels of uncertainty on  $T_{max}$ ,  
263  $T_{min}$  and  $T_{opt}$  similar to the confidence intervals presented by Bernard and Rémond [11], even  
264 if methods for uncertainty estimations were based on different approaches (Table 2).

265

### 266 3.2. Respiration rate

267 Figure 4 shows that the specific respiration rate increased exponentially with temperature over  
268 the range of temperatures tested. Similar observations were reported for a large number of  
269 algal species as reviewed by Robarts and Zohary [23]. Based on the values reported in Table  
270 1, the coefficients  $\lambda_0$  and  $\beta$  (with corresponding confidence intervals at 95%) were  $6.45 \cdot 10^{-7}$   
271  $(\pm 0.34 \cdot 10^{-7}) \text{ s}^{-1}$  and  $0.0715 (\pm 0.0002) \text{ }^\circ\text{C}^{-1}$ , respectively.

272

### 273 4. Conclusions

274 The results obtained during the model calibration performed on *D. salina* are consistent with  
275 prior observations in the literature, namely:

- 276 - The rate of gross oxygen productivity followed a typical Monod-like response to light  
277 intensity;
- 278 - The maximum specific rate of oxygen production was linearly correlated to the half-  
279 saturation constant of the Monod model, indicating that oxygen production efficiency  
280 is as expected independent of temperature at low light intensities;
- 281 - The evolutions of the maximum specific rate of photosynthesis and half-saturation  
282 constant with temperature satisfyingly fitted Bernard and Rémond's model.
- 283 - Respiration rates were shown to increase exponentially with temperature, which is  
284 consistent with prior observations in the literature.
- 285 - These results also confirm that *Dunaliella salina* can grow in a relatively wide  
286 temperature range and resist to relatively high temperatures.

287 These results indicate that the experimental technique used for model calibration is valid  
288 and that the productivity model should yield accurate predictions in outdoor cultivation  
289 systems.

290

291

292

293 Acknowledgments:

294 The authors are grateful for the support of the ANR-13-BIME-004 Purple Sun and the  
295 Inria Project Lab *Algae in silico*. Margaux Caïa (Inria BIOCORE/LOV) is acknowledged  
296 for early work on the device used for model calibration.

297

298 References

- 299 [1] Q. Béchet, A. Shilton, B. Guieysse, Modeling the effects of light and temperature on  
300 algae growth: State of the art and critical assessment for productivity prediction during  
301 outdoor cultivation, *Biotechnol. Adv.* 31 (2013) 1648–1663.
- 302 [2] E. Lee, M. Jalalizadeh, Q. Zhang, Growth kinetic models for microalgae cultivation: A  
303 review, *Algal Res.* 12 (2015) 497–512. doi:10.1016/j.algal.2015.10.004.
- 304 [3] O. Bernard, F. Mairet, B. Chachuat, Modelling of Microalgae Culture Systems with  
305 Applications to Control and Optimization, in: C. Posten, S. Feng Chen (Eds.),  
306 *Microalgae Biotechnol.*, Springer International Publishing, Cham, 2016: pp. 59–87.  
307 doi:10.1007/10\_2014\_287.
- 308 [4] P.M. Slegers, P.J.M. van Beveren, R.H. Wijffels, G. Van Straten, A.J.B. van Boxtel,  
309 Scenario analysis of large scale algae production in tubular photobioreactors, *Appl.*  
310 *Energy.* 105 (2013) 395–406. doi:10.1016/j.apenergy.2012.12.068.
- 311 [5] Q. Béchet, A. Shilton, B. Guieysse, Maximizing Productivity and Reducing  
312 Environmental Impacts of Full-Scale Algal Production through Optimization of Open  
313 Pond Depth and Hydraulic Retention Time, *Environ. Sci. Technol.* (2016)  
314 acs.est.5b05412. doi:10.1021/acs.est.5b05412.
- 315 [6] Q. Béchet, P. Chambonnière, A. Shilton, G. Guizard, B. Guieysse, Algal productivity  
316 modeling: A step toward accurate assessments of full-scale algal cultivation,  
317 *Biotechnol. Bioeng.* 112 (2015) 987–996. doi:10.1002/bit.25517.
- 318 [7] J. Benemann, Microalgae for biofuels and animal feeds, *Energies.* 6 (2013) 5869–5886.  
319 doi:10.3390/en6115869.
- 320 [8] Q. Béchet, A. Shilton, B. Guieysse, Full-scale validation of a model of algal  
321 productivity, *Environ. Sci. Technol.* 48 (2014) 13826–13833.
- 322 [9] R.R.L. Guillard, J.H. Ryther, Studies of marine planktonic diatoms: I. *Cyclotella Nana*

- 323 Hustedt and *Denotula Confervacea* (CLEVE) Gran., *Can. J. Microbiol.* 8 (1962) 229–  
324 239. doi:10.1139/m62-029.
- 325 [10] C.J. Zhu, Y.K. Lee, Determination of biomass dry weight of marine microalgae, *J.*  
326 *Appl. Phycol.* 9 (1997) 189–194. doi:10.1023/A:1007914806640.
- 327 [11] O. Bernard, B. Rémond, Bioresource Technology Validation of a simple model  
328 accounting for light and temperature effect on microalgal growth, *Bioresour. Technol.*  
329 123 (2012) 520–527. doi:10.1016/j.biortech.2012.07.022.
- 330 [12] C.D. Collins, C.W. Boylen, Physiological responses of *Anabaena variabilis*  
331 (*Cyanophyceae*) to instantaneous exposure to various combinations of light intensity  
332 and temperature, *J. Phycol.* 18 (1982) 206–211.
- 333 [13] J.U. Grobbelaar, C.J. Soeder, Respiration losses in planktonic green algae cultivated in  
334 raceway ponds, *J. Plankton Res.* 7 (1985) 497–506. doi:10.1093/plankt/7.4.497.
- 335 [14] F. Le Borgne, J. Pruvost, Investigation and modeling of biomass decay rate in the dark  
336 and its potential influence on net productivity of solar photobioreactors for microalga  
337 *Chlamydomonas reinhardtii* and cyanobacterium *Arthrospira platensis*, *Bioresour.*  
338 *Technol.* 138 (2013) 271–276. doi:10.1016/j.biortech.2013.03.056.
- 339 [15] A. Morel, Optical modeling of the upper ocean in relation to its biogenous matter  
340 content (case I waters), *J. Geophys. Res.* 93 (1988) 10749–10768.  
341 doi:10.1029/JC093iC09p10749.
- 342 [16] C.G. Hatchard, C.A. Parker, A New Sensitive Chemical Actinometer. II. Potassium  
343 Ferrioxalate as a Standard Chemical Actinometer, *Proc. R. Soc. London A Math. Phys.*  
344 *Eng. Sci.* 235 (1956) 518–536.  
345 <http://rspa.royalsocietypublishing.org/content/235/1203/518.abstract>.
- 346 [17] K. Wegmann, H. Metzner, Synchronization of *Dunaliella* cultures, *Arch. Mikrobiol.* 78  
347 (1971) 360–367. doi:10.1007/BF00412276.



- 348 [18] C. Combe, P. Hartmann, S. Rabouille, A. Talec, O. Bernard, A. Sciandra, Long-term  
349 adaptive response to high-frequency light signals in the unicellular photosynthetic  
350 eukaryote *Dunaliella salina*, *Biotechnol. Bioeng.* 112 (2015) 1111–1121.
- 351 [19] O. Bernard, Hurdles and challenges for modelling and control of microalgae for CO<sub>2</sub>  
352 mitigation and biofuel production, *J. Process Control.* 21 (2011) 1378–1389.  
353 doi:10.1016/j.jprocont.2011.07.012.
- 354 [20] I.R. Davison, Environmental effects on algal photosynthesis: temperature, *J. Phycol.* 27  
355 (1991) 2–8. doi:10.1111/j.0022-3646.1991.00002.x.
- 356 [21] L.J. Borowitzka, M.A. Borowitzka, Commercial Production of  $\beta$ -carotene by  
357 *Dunaliella salina* in open ponds, *Bull. Mar. Sci.* 47 (1990) 244–252.
- 358 [22] P.I. Gómez, M.A. González, The effect of temperature and irradiance on the growth  
359 and carotenogenic capacity of seven strains of *Dunaliella salina* (Chlorophyta)  
360 cultivated under laboratory conditions, *Biol. Res.* 38 (2005) 151–162.
- 361 [23] R.D. Robarts, T. Zohary, Temperature effects on photosynthetic capacity, respiration,  
362 and growth rates of bloom-forming cyanobacteria, *New Zeal. J. Mar. Freshw. Res.* 21  
363 (1987) 391–399. doi:10.1080/00288330.1987.9516235.
- 364

365 Table 1: Model parameters values at different temperatures (values in parenthesis indicate  
 366 confidence level at 95% estimated through Monte-Carlo simulations). Values of  $P_m$  and  $\lambda$  in  
 367 kg/kg-s can be obtained by using the conversion coefficients provided in Section 2.6. Values  
 368 of  $K$  can be obtained in  $\mu\text{mol/kg-s}$  by using a conversion factor of  $4.79 \mu\text{mol/W-s}$  (based on  
 369 the spectral distribution of device lamps shown in S1).

Temperature (°C)	3.7	10.2	19.7	27.7	34.7	40.9
$P_m$ ( $10^{-4}$ kg O <sub>2</sub> /kg-s)	0.165 (0.014)	0.571 (0.096)	1.19 (0.25)	2.08 (0.43)	1.77 (0.33)	1.35 (0.88)
$K$ ( $10^4$ W/kg)	0.479 (0.095)	2.46 (0.64)	2.79 (0.87)	4.77 (1.34)	3.34 (0.89)	3.28 (3.31)
$\lambda$ ( $10^{-6}$ kg O <sub>2</sub> /kg-s)	0.88 (0.05)	1.22 (0.06)	2.55 (0.13)	5.45 (0.28)	7.53 (0.39)	11.5 (0.6)

370

371 Table 2: Bernard and Rémond's model parameters for  $P_m$  and  $K$  (values in parenthesis indicate  
 372 confidence interval at 95% estimated through Monte-Carlo simulations) - Symbols are  
 373 defined in Equation 4. Values of  $\alpha$  for  $K$  can be obtained in  $\mu\text{mol}/\text{kg}\cdot\text{s}$  by using a conversion  
 374 factor of  $4.79 \mu\text{mol}/\text{W}\cdot\text{s}$

Parameter (unit)	$T_{min}$ ( $^{\circ}\text{C}$ )	$T_{opt}$ ( $^{\circ}\text{C}$ )	$T_{max}$ ( $^{\circ}\text{C}$ )	$\alpha$
$P_m$ (kg O <sub>2</sub> /kg-s)	-7.8 (8.4)	34.0 (3.9)	43.0 (0.1)	$2.08 \cdot 10^{-4}$ kg O <sub>2</sub> /kg-s
$K$ (W/kg)	-15.4 (17.3)	33.7 (8.0)	43.0 (0.4)	$4.77 \cdot 10^4$ W/kg

375

376 Figures

377

378 Figure 1: Gross rate of photosynthesis vs. incident light intensity at different temperatures

379 (dots: experimental data; plain lines: theoretical fitting) - Error bars represent standard

380 deviation of error caused by experimental error. Light intensities in  $\text{W}/\text{m}^2$  can be converted

381 into  $\mu\text{mol}/\text{m}^2\text{-s}$  by using a conversion factor of  $4.79 \mu\text{mol}/\text{W}\text{-s}$ .

382

383 Figure 2: Values of the maximum specific growth rate  $P_m$  vs. the half-constant  $K$  (dots:

384 experimental data; plain line: linear regression) - Error bars indicate the standard deviation

385 estimated through Monte-Carlo simulations.

386

387 Figure 3: Evolution of the maximum specific oxygen productivity and half-saturation constant

388 with temperature (dots: experimental data; plain line: fitting with Bernard and Rémond's

389 model) - Error bars represent the standard deviation estimated through Monte-Carlo

390 simulations. Values of  $K$  can be obtained in  $\mu\text{mol}/\text{kg}\text{-s}$  by using a conversion factor of  $4.79$

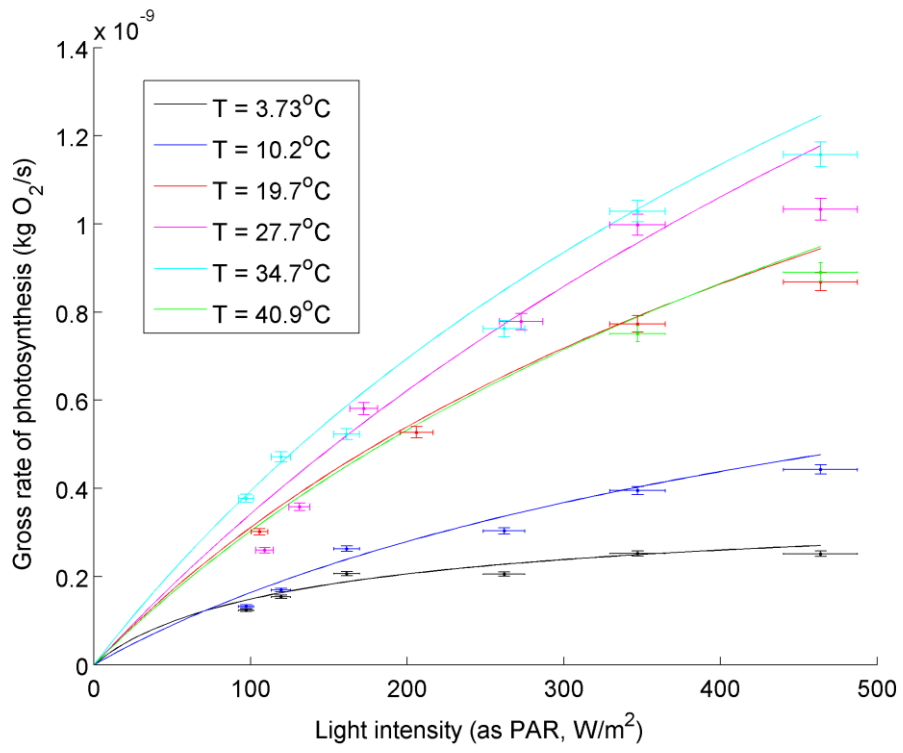
391  $\mu\text{mol}/\text{W}\text{-s}$ .

392

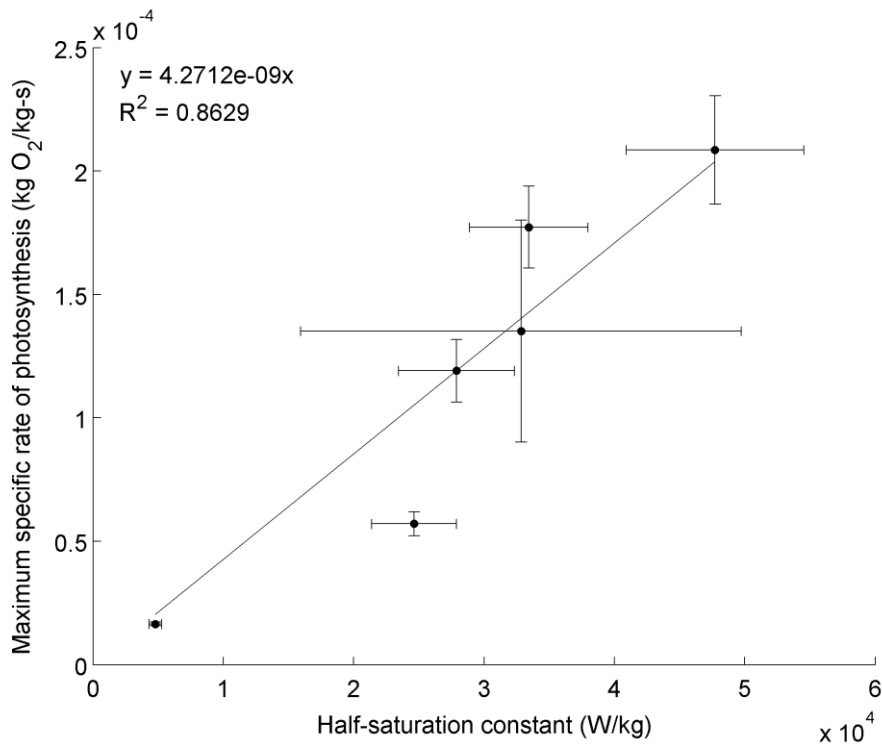
393 Figure 4: Evolution of the respiration specific rate with temperature (dots: experimental data;

394 plain line: fitting to an exponential function as described by Equation 6) - Error bars represent

395 standard deviation estimated through Monte-Carlo simulations.

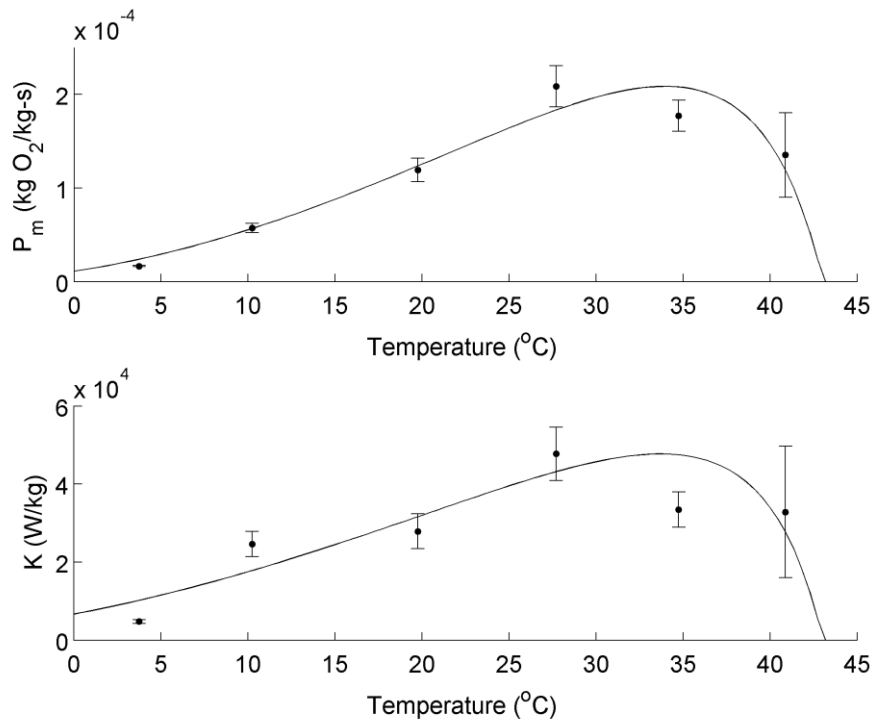


398 Figure 2



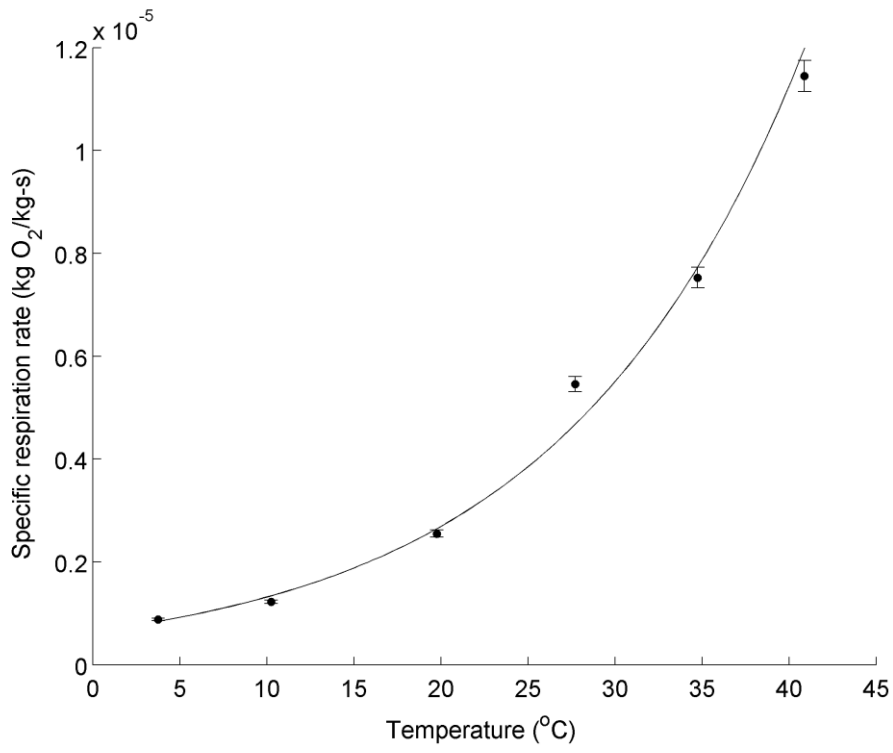
399

400 Figure 3



401

402 Figure 4



403